

Search for a light Higgs boson at *BABAR*

SWAGATO BANERJEE (ON BEHALF OF THE *BABAR* COLLABORATION)

University of Victoria, P.O. Box 3055, Victoria, B.C., CANADA V8W 3P6.

Summary. — We search for evidence of a light Higgs boson (A^0) in the radiative decays of the narrow $\Upsilon(3S)$ resonance: $\Upsilon(3S) \rightarrow \gamma A^0$, where $A^0 \rightarrow$ invisible or $A^0 \rightarrow \mu^+ \mu^-$. Such an object appears in extensions of the Standard Model, where a light CP -odd Higgs boson naturally couples strongly to b -quarks. We find no evidence for such processes in a sample of 122×10^6 $\Upsilon(3S)$ decays collected by the *BABAR* collaboration at the PEP-II B-factory, and set 90% C.L. upper limits on the product of the branching fractions $\mathcal{B}(\Upsilon(3S) \rightarrow \gamma A^0) \times \mathcal{B}(A^0 \rightarrow \text{invisible})$ at $(0.7 - 31) \times 10^{-6}$ in the mass range $m_{A^0} \leq 7.8$ GeV, and on the product $\mathcal{B}(\Upsilon(3S) \rightarrow \gamma A^0) \times \mathcal{B}(A^0 \rightarrow \mu^+ \mu^-)$ at $(0.25 - 5.2) \times 10^{-6}$ in the mass range $0.212 \leq m_{A^0} \leq 9.3$ GeV. We also set a limit on the dimuon branching fraction of the recently discovered η_b meson $\mathcal{B}(\eta_b \rightarrow \mu^+ \mu^-) < 0.8\%$ at 90% C.L. The results are preliminary.

PACS 12.60.Fr – Extensions of electroweak Higgs sector.

PACS 14.80.Cp – Non-standard-model Higgs bosons.

PACS 13.66.Fg – Gauge and Higgs boson production in $e^- e^+$ interactions.

1. – INTRODUCTION

The concept of mass is one of the most intuitive ideas in physics since it is present in everyday human experience. Yet the fundamental nature of mass remains one of the greatest mysteries in physics. The Higgs mechanism is a theoretically appealing way to account for the different masses of elementary particles [1]. The Higgs mechanism implies the existence of at least one new particle called the Higgs boson, which is the only Standard Model (SM) [2] particle yet to be observed. If it is found, its discovery will have a profound effect on our fundamental understanding of matter. A single Standard Model Higgs boson is required to be heavy, with the mass constrained by direct searches to $m_H > 114.4$ GeV [3] and $m_H \neq 170$ GeV [4], and by precision electroweak measurements to $m_H = 129^{+74}_{-49}$ GeV [5].

The Standard Model and the simplest electroweak symmetry breaking scenario suffer from quadratic divergences in the radiative corrections to the mass parameter of the Higgs potential. Several theories beyond the Standard Model that regulate these divergences have been proposed. Supersymmetry [6] is one such model; however, in its simplest

form (the Minimal Supersymmetric Standard Model, MSSM) questions of parameter fine-tuning and “naturalness” of the Higgs mass scale remain.

Theoretical efforts to solve unattractive features of MSSM often result in models that introduce additional Higgs fields, with one of them naturally light. For instance, the Next-to-Minimal Supersymmetric Standard Model (NMSSM) [7] introduces a singlet Higgs field. A linear combination of this singlet state with a member of the electroweak doublet produces a CP -odd Higgs state A^0 whose mass is not required to be large. Direct searches typically constrain m_{A^0} to be below $2m_b$ [8] making it accessible to decays of \mathcal{T} resonances. An ideal place to search for such CP -odd Higgs would be $\mathcal{T} \rightarrow \gamma A^0$, as originally proposed by Wilczek [9]. A study of the NMSSM parameter space [10] predicts the branching fraction to this final state to be as high as 10^{-4} .

Other new physics models, motivated by astrophysical observations, predict similar light states. One recent example [11] proposes a light axion-like pseudoscalar boson a decaying predominantly to leptons and predicts the branching fraction $\mathcal{B}(\mathcal{T} \rightarrow \gamma a)$ to be between 10^{-6} – 10^{-5} [11]. Empirical motivation for a light Higgs search comes from the HyperCP experiment [12]. HyperCP observed three anomalous events in the $\Sigma \rightarrow p\mu^+\mu^-$ final state, that have been interpreted as a light scalar with mass of 214.3 MeV decaying into a pair of muons [13]. The large datasets available at *BABAR* allow us to place stringent constraints on such models.

If a light scalar A^0 exists, the pattern of its decays would depend on its mass. In dark matter inspired scenarios, $A^0 \rightarrow$ invisible decays could be dominant. For low masses $m_{A^0} < 2m_\tau$, relevant for the axion [11] and HyperCP [12] interpretations, the dominant decay mode should be $A^0 \rightarrow \mu^+\mu^-$. Significantly above the tau-pair threshold, $A^0 \rightarrow \tau^+\tau^-$ would dominate, and the hadronic decays may also be significant.

Preliminary results from search for invisible Higgs decays are described in Ref. [14]. This analysis [15] searches for the radiative production of Higgs in $\mathcal{T}(3S)$ decays, which subsequently decays into muons:

$$\mathcal{T}(3S) \rightarrow \gamma A^0; A^0 \rightarrow \mu^+\mu^-$$

The current best limit on the branching fraction $\mathcal{B}(\mathcal{T} \rightarrow \gamma A^0)$ with $A^0 \rightarrow \mu^+\mu^-$ comes from a measurement by the CLEO collaboration on $\mathcal{T}(1S)$ [16]. The quoted limits on $\mathcal{B}(\mathcal{T}(1S) \rightarrow \gamma A^0) \times \mathcal{B}(A^0 \rightarrow \mu^+\mu^-)$ are in the range $(1-20) \times 10^{-6}$ for $m_{A^0} < 3.6$ GeV. There are currently no competitive measurements at the higher-mass \mathcal{T} resonances or for the values of m_{A^0} above the $\tau\tau$ threshold.

In the following, we describe a search for a resonance in the dimuon invariant mass distribution for fully reconstructed final state $\mathcal{T}(3S) \rightarrow \gamma(\mu^+\mu^-)$. We assume that the decay width of the resonance is negligibly small compared to experimental resolution, as expected [11, 17] for m_{A^0} sufficiently far from the mass of the η_b [18]. We also assume that the resonance is a scalar (or pseudo-scalar) particle; while significance of any peak does not depend on this assumption, the signal efficiency and, therefore, the extracted branching fractions are computed for a spin-0 particle. In addition, following the recent discovery of the η_b meson in $\mathcal{T}(3S)$ decays [18], we look for the leptonic decay of the η_b through the chain $\mathcal{T}(3S) \rightarrow \gamma\eta_b, \eta_b \rightarrow \mu^+\mu^-$. If the recently discovered state is the conventional quark-antiquark η_b meson, its leptonic width is expected to be negligible. Thus, setting a limit on the dimuon branching fraction sheds some light on the nature of the recently discovered state. We assume $\Gamma(\eta_b) = 10$ MeV, which is expected in most theoretical models and is consistent with *BABAR* results [18].

2. – THE *BABAR* DETECTOR AND DATASET

We search for two-body transitions $\Upsilon(3S) \rightarrow \gamma A^0$, followed by the decay $A^0 \rightarrow$ invisible [14] or $A^0 \rightarrow \mu^+\mu^-$ [15] in a sample of $(121.8 \pm 1.2) \times 10^6$ $\Upsilon(3S)$ decays collected with the *BABAR* detector at the PEP-II asymmetric-energy e^+e^- collider at the Stanford Linear Accelerator Center. The data were collected at the nominal center-of-mass (CM) energy $E_{\text{cm}} = 10.355$ GeV. The CM frame was boosted relative to the detector approximately along the detector’s magnetic field axis by $\beta_z = 0.469$.

We use a sample of 78.5 fb^{-1} accumulated on $\Upsilon(4S)$ resonance ($\Upsilon(4S)$ sample) for studies of the continuum backgrounds; since $\Upsilon(4S)$ is three orders of magnitude broader than $\Upsilon(3S)$, the branching fraction $\Upsilon(4S) \rightarrow \gamma A^0$ is expected to be negligible. For characterization of the background events and selection optimization we also use a sample of 2.4 fb^{-1} collected 30 MeV below the $\Upsilon(3S)$ resonance.

The *BABAR* detector is described in detail elsewhere [19]. We use the GEANT4 [20] software to simulate interactions of particles traversing the *BABAR* detector, taking into account the varying detector conditions and beam backgrounds.

3. – EVENT SELECTION FOR $A^0 \rightarrow \mu^+\mu^-$ DECAYS

We select events with exactly two oppositely-charged tracks and a single energetic photon with a CM energy $E_\gamma^* \geq 0.5$ GeV. We allow other photons to be present in the event as long as their CM energies are below 0.5 GeV. We assign a muon mass hypothesis to the two tracks (henceforth referred to as muon candidates), and require that they form a geometric vertex with the $\chi_{\text{vtx}}^2 < 20$ (for 1 degree of freedom), displaced transversely by at most 2 cm from the nominal location of the e^+e^- interaction region. We perform a kinematic fit to the $\Upsilon(3S)$ candidate formed from the two muon candidates and the energetic photon, constraining the CM energy of the $\Upsilon(3S)$ candidate, within the beam energy spread, to the total beam energy \sqrt{s} . We also assume that the $\Upsilon(3S)$ candidate originates from the interaction region. The kinematic fit improves the invariant mass resolution of the muon pair. We place a requirement on the kinematic fit $\chi_{\Upsilon(3S)}^2 < 39$ (for 6 degrees of freedom), which corresponds to the probability to reject good kinematic fits of less than 10^{-6} . The kinematic fit χ^2 , together with a requirement that the total mass of the $\Upsilon(3S)$ candidate is within 2 GeV of \sqrt{s} , suppresses background events with more than two muons and a photon in the final state, such as cascade decays $\Upsilon(3S) \rightarrow \gamma \chi_b(2P) \rightarrow \gamma \gamma \Upsilon(1S) \rightarrow \gamma \gamma \mu^+ \mu^-$ etc. We further require that the momentum of the dimuon candidate A^0 and the photon direction are back-to-back in the CM frame to within 0.07 radians, and select events in which the cosine of the angle between the muon direction and A^0 direction in the center of mass of A^0 is less than 0.88. We reject events in which neither muon candidate is positively identified in the muon chamber.

The kinematic selection described above is highly efficient for signal events. After the selection, the backgrounds are dominated by two types of QED processes: “continuum” $e^+e^- \rightarrow \gamma \mu^+ \mu^-$ events in which a photon is emitted in the initial or final state, and the initial-state radiation (ISR) production of the vector mesons J/ψ , $\psi(2S)$, and $\Upsilon(1S)$, which subsequently decay into muon pairs. In order to suppress contributions from ISR-produced $\rho^0 \rightarrow \pi^+\pi^-$ and $\phi \rightarrow K^+K^-$ final states in which a pion or a kaon is misidentified as a muon or decays (*e.g.* through $K^+ \rightarrow \mu^+\nu_\mu$), we require that both muons are positively identified when we look for A^0 candidates in the range $m_{A^0} < 1.05$ GeV. Finally, when selecting candidate events in the η_b mass region $m_{\mu\mu} \sim 9.39$ GeV, we require that no secondary photon above a CM energy of $E_2^* = 0.08$ GeV is present in

the event; this requirement suppresses decay chains $\Upsilon(3S) \rightarrow \gamma_2 \chi_b(2S) \rightarrow \gamma_1 \gamma_2 \Upsilon(1S)$, in which the photon γ_2 has a typical CM energy of 100 MeV.

We use Monte Carlo samples generated at 20 values of m_{A^0} over a broad range $0.212 < m_{A^0} \leq 9.5 \text{ GeV}$ of possible A^0 masses to measure selection efficiency for the signal events. The efficiency varies between 24-44%, depending on the dimuon invariant mass.

4. – EXTRACTION OF SIGNAL YIELDS FOR $A^0 \rightarrow \mu^+ \mu^-$ DECAYS

The invariant mass spectrum for the selected candidates in the $\Upsilon(3S)$ dataset is shown in Fig. 1 (left). We extract the yield of signal events as a function of the assumed mass m_{A^0} in the interval $0.212 \leq m_{A^0} \leq 9.3 \text{ GeV}$ by performing a series of unbinned extended maximum likelihood fits to the distribution of the “reduced mass”

$$(1) \quad m_R = \sqrt{m_{\mu\mu}^2 - 4m_\mu^2}.$$

The choice of this variable is motivated by the distribution of the *continuum background* from $e^+e^- \rightarrow \gamma\mu^+\mu^-$, which is a smooth function of m_R across the entire range of interest, in particular, the region near the kinematic threshold $m_{\mu\mu} \approx 2m_\mu$ ($m_R \approx 0$). Each fit is performed over a small range of m_R around the value expected for a particular m_{A^0} . We use the $\Upsilon(4S)$ sample to determine the probability density functions (PDFs) for the continuum background in each fit window, which agree within statistical uncertainties with Monte Carlo simulations. We use a threshold (hyperbolic) function to describe the background below $m_R < 0.23 \text{ GeV}$; its parameters are fixed to the values determined from the fits to the $\Upsilon(4S)$ dataset. Elsewhere the background is well described in each limited m_R range by a first-order ($m_R < 9.3 \text{ GeV}$) or second-order ($m_R > 9.3 \text{ GeV}$) polynomial.

The signal PDF is described by a sum of two Crystal Ball functions [21] with tail parameters on either side of the maximum. The signal PDFs are centered around the expected values of $m_R = \sqrt{m_{A^0}^2 - 4m_\mu^2}$ and have the typical resolution of 2 – 10 MeV, which increases monotonically with m_{A^0} . We determine the PDF as a function of m_{A^0} using a set of high-statistics simulated samples of signal events, and we interpolate PDF parameters and signal efficiency values linearly between simulated points. We determine the uncertainty in the PDF parameters by comparing the distributions of the simulated and reconstructed $e^+e^- \rightarrow \gamma_{\text{ISR}} J/\psi$, $J/\psi \rightarrow \mu^+\mu^-$ events.

Known resonances, such as J/ψ , $\psi(2S)$, and $\Upsilon(1S)$, are present in our sample in specific intervals of m_R , and constitute *peaking background*. We include these contributions in the fit where appropriate, and describe the shape of the resonances using the same functional form as for the signal, a sum of two Crystal Ball functions, with parameters determined from the dedicated MC samples. We do not search for A^0 signal in the immediate vicinity of J/ψ and $\psi(2S)$, ignoring the region of $\approx \pm 40 \text{ MeV}$ around J/ψ (approximately $\pm 5\sigma$) and $\approx \pm 25 \text{ MeV}$ ($\approx \pm 3\sigma$) around $\psi(2S)$.

For each assumed value of m_{A^0} , we perform a likelihood fit to the m_R distribution under the following conditions:

- $0.212 \leq m_{A^0} < 0.5 \text{ GeV}$: we use a fixed interval $0.01 < m_R < 0.55 \text{ GeV}$. The fits are done in 2 MeV steps in m_{A^0} . We use a threshold function to describe the combinatorial background PDF below $m_R < 0.23 \text{ GeV}$, and constrain it to the

shape determined from the large $\Upsilon(4S)$ dataset. For $m_R > 0.23$ GeV, we describe the background by a first-order Chebyshev polynomial and float its shape, while requiring continuity at $m_R = 0.23$ GeV. Signal and background yields are free parameters in the fit.

- $0.5 \leq m_{A^0} < 1.05$ GeV: we use sliding intervals $\mu - 0.2 < m_R < \mu + 0.1$ GeV (where μ is the mean of the signal distribution of m_R). We perform fits in 3 MeV steps in m_{A^0} . First-order polynomial coefficient of the background PDF, signal and background yields are free parameters in the fit.
- $1.05 \leq m_{A^0} < 2.9$ GeV: we use sliding intervals $\mu - 0.2 < m_R < \mu + 0.1$ GeV and perform fits in 5 MeV steps in m_{A^0} . First-order polynomial coefficient of the background PDF, signal and background yields are free parameters in the fit.
- $2.9 \leq m_{A^0} \leq 3.055$ GeV and $3.135 \leq m_{A^0} \leq 3.395$ GeV: we use a fixed interval $2.7 < m_R < 3.5$ GeV; 5 MeV steps in m_{A^0} . First-order polynomial coefficient of the background PDF, signal, J/ψ , and background yields are free parameters in the fit.
- $3.4 \leq m_{A^0} < 3.55$ GeV: we use sliding intervals $\mu - 0.2 < m_R < \mu + 0.1$ GeV and perform fits in 5 MeV steps in m_{A^0} . First-order polynomial coefficient of the background PDF, signal and background yields are free parameters in the fit.
- $3.55 \leq m_{A^0} \leq 3.66$ GeV and $3.71 \leq m_{A^0} < 4.0$ GeV: we use fixed interval $3.35 < m_R < 4.1$ GeV; 5 MeV steps in m_{A^0} . First-order polynomial coefficient of the background PDF, signal, $\psi(2S)$, and background yields are free parameters in the fit.
- $4.0 \leq m_{A^0} < 9.3$ GeV: we use sliding intervals $\mu - 0.2 < m_R < \mu + 0.1$ GeV; 5 MeV steps in m_{A^0} . First-order polynomial coefficient of the background PDF, signal and background yields are free parameters in the fit.
- η_b region ($m_{\eta_b} = 9.390$ GeV): we use a fixed interval $9.2 < m_R < 9.6$ GeV. We constrain the contribution from $e^+e^- \rightarrow \gamma_{\text{ISR}}\Upsilon(1S)$ to the expectation from the $\Upsilon(4S)$ dataset (436 ± 50 events). Background PDF shape (second-order Chebyshev polynomial), yields of $\Upsilon(3S) \rightarrow \gamma\chi_b(2P) \rightarrow \gamma\gamma\Upsilon(1S)$, signal $\Upsilon(3S) \rightarrow \gamma\eta_b$ events, and background yields are free parameters in the fit.

The step sizes in each interval correspond approximately to the resolution in m_{A^0} .

5. – SYSTEMATIC UNCERTAINTIES for $A^0 \rightarrow \mu^+\mu^-$

The largest systematic uncertainty in $\mathcal{B}(\Upsilon(3S) \rightarrow \gamma A^0)$ comes from the measurement of the selection efficiency. We compare the overall selection efficiency between the data and the Monte Carlo simulation by measuring the absolute cross section $d\sigma/dm_R$ for the radiative QED process $e^+e^- \rightarrow \gamma\mu^+\mu^-$ over the broad kinematic range $0 < m_R \leq 9.6$ GeV, using a sample of 2.4fb^{-1} collected 30 MeV below the $\Upsilon(3S)$. We use the ratio of measured to expected cross sections to correct the signal selection efficiency as a function of m_{A^0} . This correction reaches up to 20% at low values of m_{A^0} . We use half of the applied correction, or its statistical uncertainty of 2%, whichever is larger, as the systematic uncertainty on the signal efficiency. This uncertainty accounts for effects of selection efficiency, reconstruction efficiency (for both charged tracks and the photon),

trigger efficiency, and the uncertainty in estimating the integrated luminosity. We find the largest difference between the data and Monte Carlo simulation in modeling of muon identification efficiency.

We determine the uncertainty in the signal and peaking background PDFs by comparing the data and simulated distributions of $e^+e^- \rightarrow \gamma_{\text{ISR}}J/\psi$ events. We correct for the observed 24% difference (5.3 MeV in the simulations versus 6.6 MeV in the data) in the width of the m_R distribution for these events, and use half of the correction to estimate the systematic uncertainty on the signal yield. This is the dominant systematic uncertainty on the signal yield for $m_{A^0} > 0.4$ GeV. Likewise, we find that changes in the tail parameters of the Crystal Ball PDF describing the J/ψ peak lead to variations in event yield of less than 1%. We use this estimate as a systematic error in the signal yield due to uncertainty in tail parameters.

We find excellent agreement in the shape of the continuum background distributions for $m_R < 0.23$ GeV between $\Upsilon(3S)$ and $\Upsilon(4S)$ data. We determine the PDF in the fits to $\Upsilon(4S)$ data, and propagate their uncertainties to the $\Upsilon(3S)$ data, where these contributions do not exceed $\sigma(\mathcal{B}) = 0.3 \times 10^{-6}$. For the higher masses $m_R > 0.23$ GeV, the background PDF parameters are floated in the likelihood fit.

We test for possible bias in the fitted value of the signal yield with a large ensemble of pseudo-experiments. For each experiment, we generate a sample of background events according to the number and the PDF observed in the data, and add a pre-determined number of signal events from fully-reconstructed signal Monte Carlo samples. The bias is consistent with zero for all values of m_{A^0} , and we assign a branching fraction uncertainty of $\sigma(\mathcal{B}) = 0.02 \times 10^{-6}$ at all values of m_{A^0} to cover the statistical variations in the results of the test.

The uncertainties in PDF parameters of both signal and background and the bias uncertainty affect the signal yield (and therefore significance of any peak); signal efficiency uncertainty does not. The effect of the systematic uncertainties on the signal yield is generally small. The statistical and systematic uncertainties on the branching fraction $\mathcal{B}(\Upsilon(3S) \rightarrow \gamma A^0)$ as a function of m_{A^0} are shown in Fig. 1 (right).

6. – RESULTS for $A^0 \rightarrow \mu^+\mu^-$

For a small number of fits in the scan over the $\Upsilon(3S)$ dataset, we observe local likelihood ratio values \mathcal{S} of about 3σ . The most significant peak is at $m_{A^0} = 4.940 \pm 0.003$ GeV (likelihood ratio value $\mathcal{S} = 3.0$, including systematics; $\mathcal{B} = (1.9 \pm 0.7 \pm 0.1) \times 10^{-6}$). The second most-significant peak is at $m_{A^0} = 0.426 \pm 0.001$ GeV (likelihood ratio value $\mathcal{S} = 2.9$, including systematics; $\mathcal{B} = (3.1 \pm 1.1 \pm 0.3) \times 10^{-6}$). The peak at $m_{A^0} = 4.940$ GeV is theoretically disfavored (since it is significantly above the τ threshold), while the peak at $m_{A^0} = 0.426$ GeV is in the range predicted by the axion model [11]. However, since our scans have $\mathcal{O}(2000)$ m_{A^0} points, we should expect several statistical fluctuations at the level of $\mathcal{S} \approx 3$, even for a null signal hypothesis. At least 80% of our pseudo-experiments contain a fluctuation with $\mathcal{S} = 3\sigma$ or more. Taking this into account, we conclude that neither of the above-mentioned peaks are significant.

Since we do not observe a significant excess of events above the background in the range $0.212 < m_{A^0} \leq 9.3$ GeV, we set upper limits on the branching fraction $\mathcal{B}(\Upsilon(3S) \rightarrow \gamma A^0) \times \mathcal{B}(A^0 \rightarrow \mu^+\mu^-)$. We add statistical and systematic uncertainties (which include the additive errors on the signal yield and multiplicative uncertainties on the signal efficiency and the number of recorded $\Upsilon(3S)$ decays) in quadrature. The 90% C.L. Bayesian upper limits, computed with a uniform prior and assuming a Gaussian likelihood

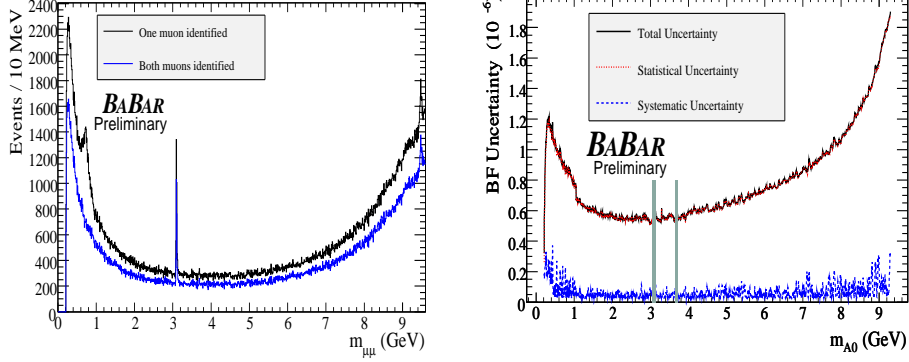


Fig. 1. – Distribution of the dimuon invariant mass $m_{\mu^+\mu^-}$ in the $\Upsilon(3S)$ data is shown on the left. Statistical and systematic uncertainty on the product of branching fractions $\mathcal{B}(\Upsilon(3S) \rightarrow \gamma A^0) \times \mathcal{B}(A^0 \rightarrow \mu^+\mu^-)$ are shown on the right as a function of m_{A^0} , extracted from the fits to the $\Upsilon(3S)$ data. Statistical errors are shown as red dot-dashed line, systematic uncertainties are shown as blue dotted line, and the total uncertainty, computed as a quadrature sum of statistical and systematic errors, is the solid black line. The shaded areas show the regions around the J/ψ and $\psi(2S)$ resonances excluded from the search.

function, are shown in Fig. 2 (right), as a function of mass m_{A^0} . The limits fluctuate depending on the central value of the signal yield returned by a particular fit, and range from 0.25×10^{-6} to 5.2×10^{-6} .

We do not observe any significant signal at the HyperCP mass, $m_{A^0} = 0.214$ GeV. We find $\mathcal{B}(\Upsilon(3S) \rightarrow \gamma A^0(214)) = (0.12^{+0.43}_{-0.41} \pm 0.17) \times 10^{-6}$, and set an upper limit $\mathcal{B}(\Upsilon(3S) \rightarrow \gamma A^0(214)) < 0.8 \times 10^{-6}$ at 90% C.L.

From a fit to the η_b region, we find $\mathcal{B}(\Upsilon(3S) \rightarrow \gamma \eta_b) \times \mathcal{B}(\eta_b \rightarrow \mu^+\mu^-) = (0.2 \pm 3.0 \pm 0.9) \times 10^{-6}$, consistent with zero. Taking into account the *BABAR* measurement of $\mathcal{B}(\Upsilon(3S) \rightarrow \gamma \eta_b) = (4.8 \pm 0.5 \pm 1.2) \times 10^{-4}$, we can derive $\mathcal{B}(\eta_b \rightarrow \mu^+\mu^-) = (0.0 \pm 0.6 \pm 0.2)\%$, or an upper limit $\mathcal{B}(\eta_b \rightarrow \mu^+\mu^-) < 0.8\%$ at 90% C.L. This is consistent with expectations from the quark model. All results above are preliminary.

The limits we set [15] are more stringent than those recently reported by the CLEO collaboration [16]. Our limits rule out much of the parameter space allowed by the light Higgs [10] and axion [11] models.

7. – CONCLUSIONS

We find no evidence for light Higgs boson in a sample of 122×10^6 $\Upsilon(3S)$ decays collected by the *BABAR* collaboration at the PEP-II B-factory, and set 90% C.L. upper limits on the product of the branching fractions $\mathcal{B}(\Upsilon(3S) \rightarrow \gamma A^0) \times \mathcal{B}(A^0 \rightarrow \text{invisible})$ at $(0.7 - 31) \times 10^{-6}$ in the mass range $m_{A^0} \leq 7.8$ GeV [14] and on the product $\mathcal{B}(\Upsilon(3S) \rightarrow \gamma A^0) \times \mathcal{B}(A^0 \rightarrow \mu^+\mu^-)$ at $(0.25 - 5.2) \times 10^{-6}$ in the mass range $0.212 \leq m_{A^0} \leq 9.3$ GeV [15]. We also set a limit on the dimuon branching fraction of the recently discovered η_b meson $\mathcal{B}(\eta_b \rightarrow \mu^+\mu^-) < 0.8\%$ at 90% C.L. [15]. The results are preliminary.

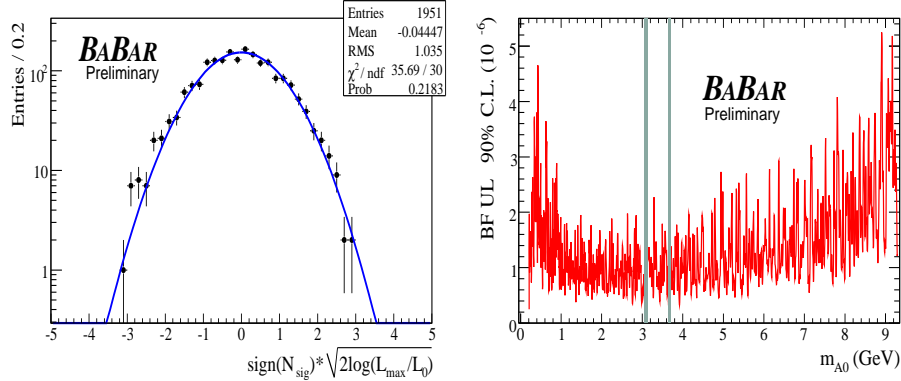


Fig. 2. – Distribution of the likelihood ratio variable \mathcal{S} with additive systematic uncertainties included for the fits to the $\Upsilon(3S)$ dataset, overlaid with a blue curve showing the Gaussian fit with fixed $\mu = 0$ and $\sigma = 1$, is shown on the left. Upper limits on the product of branching fractions $\mathcal{B}(\Upsilon(3S) \rightarrow \gamma A^0) \times \mathcal{B}(A^0 \rightarrow \mu^+ \mu^-)$ as a function of m_{A^0} from the fits to $\Upsilon(3S)$ data are shown on the right. The shaded areas show the regions around the J/ψ and $\psi(2S)$ resonances excluded from the search.

REFERENCES

- [1] P.W. Higgs Phys. Rev. Lett. **13**, 508 (1964).
- [2] S. Weinberg, Phys. Rev. Lett. **19**, 1264 (1967); A. Salam, p. 367 of *Elementary Particle Theory*, ed. N. Svartholm (Almqvist and Wiksells, Stockholm, 1969); S.L. Glashow, J. Iliopoulos, and L. Maiani, Phys. Rev. D **2**, 1285 (1970).
- [3] LEP Working Group for Higgs boson searches, R. Barate *et al.*, Phys. Lett. **B565**, 61 (2003).
- [4] M. Herndon, rapporteur talk at ICHEP '08, arXiv:0810.3705 [hep-ex] (2008).
- [5] LEP-SLC Electroweak Working Group, Phys. Rept. **427**, 257 (2006).
- [6] J. Wess and B. Zumino, Nucl. Phys. **B70**, 39 (1974).
- [7] R. Dermisek and J.F. Gunion, Phys. Rev. Lett. **95**, 041801 (2005).
- [8] R. Dermisek and J.F. Gunion, Phys. Rev. D **73**, 111701 (2006).
- [9] F. Wilczek, Phys. Rev. Lett. **39**, 1304 (1977).
- [10] R. Dermisek, J.F. Gunion, and B. McElrath, Phys. Rev. D **76**, 051105 (2007).
- [11] Y. Nomura and J. Thaler, preprint arXiv:0810.5397 [hep-ph] (2008).
- [12] H. Park *et al.*, HyperCP Collaboration, Phys. Rev. Lett. **94**, 021801 (2005).
- [13] X. G. He, J. Tandean and G. Valencia, Phys. Rev. Lett. **98**, 081802 (2007).
- [14] B. Aubert *et al.*, BABAR Collaboration, arXiv:0808.0017 [hep-ex].
- [15] B. Aubert *et al.*, BABAR Collaboration, arXiv:0902.2176 [hep-ex].
- [16] W. Love, *et al.*, CLEO Collaboration, Phys. Rev. Lett. **101**, 151802 (2008).
- [17] E. Fullana and M.A. Sanchis-Lozano, Phys. Lett. B **653**, 67 (2007).
- [18] B. Aubert *et al.*, BABAR Collaboration, Phys. Rev. Lett. **101**, 071801 (2008).
- [19] B. Aubert *et al.*, BABAR Collaboration, Nucl. Instrum. Methods Phys. Res., Sect. A **479**, 1 (2002).
- [20] S. Agostinelli *et al.*, GEANT4 Collaboration, Nucl. Instrum. Methods Phys. Res., Sect. A **506**, 250 (2003).
- [21] M. J. Oreglia, Ph.D Thesis, report SLAC-236 (1980), Appendix D; J. E. Gaiser, Ph.D Thesis, report SLAC-255 (1982), Appendix F; T. Skwarnicki, Ph.D Thesis, report DESY F31-86-02(1986), Appendix E.